# A possible periodic RM evolution in the repeating FRB 20220529

YI-FANG LIANG,  $^{1,2}$  YE LI,  $^1$  ZHEN-FAN TANG,  $^{1,2}$  XUAN YANG,  $^1$  SONG-BO ZHANG,  $^1$  YUAN-PEI YANG,  $^{3,1}$  FA-YIN WANG,  $^{4,5}$  BAO WANG,  $^{1,2}$  DI XIAO,  $^1$  QING ZHAO,  $^{1,2}$  JUN-JIE WEI,  $^{1,2}$  JIN-JUN GENG,  $^1$  JIA-RUI NIU,  $^6$  JUN-SHUO ZHANG,  $^{6,7}$  GUO CHEN,  $^1$  MIN FANG,  $^1$  XUE-FENG WU,  $^{1,2}$  ZI-GAO DAI,  $^{8,2}$  WEI-WEI ZHU,  $^6$  PENG JIANG,  $^6$  AND BING ZHANG ZHANG  $^{10,11}$ 

<sup>1</sup>Purple Mountain Observatory, Chinese Academy of Sciences, Nanjing 210008, China
<sup>2</sup>School of Astronomy and Space Sciences, University of Science and Technology of China, Hefei 230026, China
<sup>3</sup>South-Western Institute for Astronomy Research, Yunnan University, Kunming 650504, China
<sup>4</sup>School of Astronomy and Space Science, Nanjing University, Nanjing 210093, China
<sup>5</sup>Key Laboratory of Modern Astronomy and Astrophysics (Nanjing University), Ministry of Education, Nanjing 210093, China

<sup>6</sup>National Astronomical Observatories, Chinese Academy of Sciences, 20A Datun Road, Chaoyang District, Beijing 100101, People's Republic of China

<sup>7</sup>School of Astronomy and Space Science, University of Chinese Academy of Sciences, Beijing 100049, People's Republic of China Bepartment of Astronomy, University of Science and Technology of China, Hefei 230026, People's Republic of China CAS Key Laboratory of FAST, National Astronomical Observatories, Chinese Academy of Sciences, Beijing 100101, People's Republic of China

<sup>10</sup> The Nevada Center for Astrophysics, University of Nevada, Las Vegas, NV 89154, USA
 <sup>11</sup> Department of Physics and Astronomy, University of Nevada, Las Vegas, NV 89154, USA

#### ABSTRACT

Fast radio bursts (FRBs) are mysterious millisecond-duration radio transients from the distant universe. Some of them repeat, while others do not. In order to explore their origin, periodic examinations have been conducted on repeating FRBs. Most of them show irregular properties, including burst rate, dispersion measure (DM), and rotation measure (RM). A notable exception is FRB 20180916B, which shows a significant 16-day periodic burst rate. Possible periodic activities have also been reported in FRB 20121102A and FRB 20240209A. However, periodic studies of other properties are sparse. FRB 20220529 was monitored by the Five-hundred-meter Aperture Spherical radio Telescope (FAST) for nearly three years, enabling periodic examinations of its properties. Here we report a possible period of  $\sim$  200 days in the RM evolution, with a significance of 4.2  $\sigma$  estimated via the Lomb-Scargle algorithm and 3.5  $\sigma$  with a phase-folding method. The burst rate was also examined for periodicity. This is consistent with the binary origin indicated by the significant RM increase and its prompt recovery.

# 1. INTRODUCTION

FRBs are extragalactic radio transients with durations on the order of milliseconds (ms) (Lorimer et al. 2007; Thornton et al. 2013), see (Zhang 2023) for a review). Many theoretical models have been proposed to explain FRBs (see (Katz 2016; Platts et al. 2019) for theoretical reviews<sup>1</sup>), with most of them invoking neutron stars or other compact objects (e.g., black holes or white dwarfs). To date, more than 1000 FRBs have been reported. Among them, around 60 are known to repeat (The CHIME/FRB Collaboration et al. 2019; Chime/Frb Collaboration et al. 2023), exhibiting burst counts ranging from 2 to over 10000 (Li et al. 2021; Xu

Corresponding author: Ye Li, Xuan Yang, Xue-Feng Wu yeli@pmo.ac.cn; yangxuan@pmo.ac.cn; xfwu@pmo.ac.cn

et al. 2022; Niu et al. 2022; Zhou et al. 2022; Zhang et al. 2023; Zhou et al. 2025), others appear non-repeating (Spitler et al. 2016; Li et al. 2021). The evolution of repeating FRB properties, such as burst rate, dispersion measure (DM), and rotation measure (RM), provides invaluable diagnostics of their progenitors and local environments. While most of them seem to be irregular, a few repeating FRBs show interesting properties.

Observations of repeating FRBs have revealed periodic activity in a few sources, while others seem not. The first FRB reported to be periodically active is FRB 20180916B, which exhibits a well-established period of 16.35 days (Amiri et al. 2020). The active phase has been further reported to be frequency-dependent (Pastor-Marazuela et al. 2021). In addition, a possible period of approximately 160 days has been reported in the active repeater FRB 20121102A (Rajwade et al. 2020; Cruces et al. 2020; Braga et al. 2025). Recently, a candidate period of 126 days was reported in the ac-

<sup>&</sup>lt;sup>1</sup> https://frbtheorycat.org/index.php/Main\_Page

tivity of FRB 20240209A (Pal 2025). These discoveries highlight the diversity in the recurrence timescales and modes of repeating FRBs. The presence of periodicity in a few repeaters suggests that at least some FRBs may originate from binary systems (Ioka & Zhang 2020; Wada et al. 2021) or undergo precessing motion (Levin et al. 2020).

If FRBs are from binary systems, periodic variation of other properties, such as RM, is also expected (Wang et al. 2022; Zhang 2018; Yang et al. 2023). Physically. RM quantifies the convolution of electron density and magnetic field along the line of sight, serving as a diagnostic of the magneto-ionic environment surrounding an FRB source. This measurement provides valuable insights into the physical conditions of the medium through which the burst propagates. For FRB 20180916B, the RM exhibits stochastic fluctuations around  $-114 \text{ rad m}^{-2}$  before MJD 59300. Then, it nearly linearly changes to -50 rad m<sup>-2</sup> from MJD 59300 to 59700, followed by random variations until 60352 (Bethapudi et al. 2025). Notably, this RM evolution lacks periodicity correlated with the source's burst activity cycle. Potential explanations include the expansion of a supernova remnant or turbulent plasma fluctuations in the vicinity of the FRB (Yang et al. 2023). A binary system explanation of the RM would require a periodicity inconsistent with current burst rate estimates(Zhao et al. 2023). The RMs in FRB 20121102A have absolute values as high as  $\sim 10^5$  rad m<sup>-2</sup>. Longterm monitoring has revealed a decreasing RM trend accompanied by some fluctuations (Michilli et al. 2018; Hilmarsson et al. 2021). Similar to 20180916B, no periodic RM evolution has been detected. The RM evolution of FRB 20121102A may be attributed to a supernova remnant or the wind nebula surrounding the FRB progenitor. Additional RM studies of other repeating FRBs have also provided important insights into the origins of FRBs. For instance, irregular variations have been observed in FRB 20201124A (Xu et al. 2022), while a sign reversal in RM has been detected in FRB 20190520B (Anna-Thomas et al. 2023). Nevertheless, periodic studies of RM are sparse <sup>2</sup>.

FRB 20220529 is another repeating FRB that may be associated with a binary system. It was first detected by the Canadian Hydrogen Intensity Mapping Experiment (CHIME) on May 29, 2022, and was identified as a repeating FRB originating from a disk galaxy at a redshift of 0.1839. We monitored it using the Five-hundred-meter Aperture Spherical radio Telescope (FAST) and the Parkes telescope for nearly three years. It shows an abrupt increase in RM to  $\sim 2000\,\mathrm{rad}\,\mathrm{m}^{-2}$  and prompt recovery of RM within two weeks, against a baseline of

 $17 \pm 101 \,\mathrm{rad}\,\mathrm{m}^{-2}$  for more than 1.5 years, strongly supporting a binary origin (Li et al. 2025). The continuous detection of pulses in FRB 20220529 enables us to examine the periodicity of its properties more efficiently.

In this work, we perform a periodicity search for the RM evolution of FRB 20220529, which spans approximately 1000 days. Using both the Lomb-Scargle Periodogram (LSP) method and the period-folding analysis, we investigate potential periodic modulation in the RM variations of this actively repeating FRB. The paper is structured as follows. The observations and data reductions of FRB 20220529 are presented in Section 2. The periodicity examinations of its RM are presented in Section 3. The implications of our results are discussed in Section 4, and we conclude in Section 5.

#### 2. OBSERVATIONS AND DATA REDUCTION

FRB 20220529 was discovered by the CHIME telescope, and was reported to repeat in June 2022. It has been monitored with the FAST telescope since June 22, 2022. Besides the four-grid observations on June 22, August 14, and August 17, 2022, as well as an off-beam tracking observation on August 28, 2022, FRB 20220529 was observed in tracking mode with the center beam of the FAST telescope, covering a frequency range of 1000-1500 MHz with 4096 channels. Up to April 1st, 2025, 125 observations totaling 58.4 hours were conducted with FAST, including 52.4 hours of on-source tracking. Li et al. (2025) reported the observations before September 5th, 2024. Here we summarize the FAST observations from September 5th, 2024 to April 1st, 2025 in Table 1. During this time, 4.5 hours of exposures in 13 observations were conducted.

Data collected from FAST were analyzed using two independent searching pipelines built upon the pulsar/FRB single-pulse searching packages PRESTO (Ransom 2001) and HEIMDALL (Petroff et al. 2015), which processed the full-band data. The DM was searched over the range of 200–300 pc cm<sup>-3</sup> with a step size of 0.1 pc cm<sup>-3</sup>. Single-pulse candidates with signal-tonoise ratios (S/N) greater than 7 were retained and manually verified. A total of 1169 bursts were detected, with 1094 occurring when the observations were on source. The 13 bursts detected from September 5, 2024 to April 1st, 2025 were presented in Table 1. After October 21, 2024, only one burst was detected, which was on February 22, 2025.

After being dedispersed at the detection DM with the maximum S/N, the polarization data were calibrated using the PSRCHIVE software package, with differential gain and phase corrections applied via a noise diode signal injected prior to each observation. The RM value of each burst was obtained using the RMFIT program by searching for the peak of the linear polarization intensity,  $L=\sqrt{Q^2+U^2}$ , within the range of -4000 to +4000 rad m<sup>-2</sup> with a step size of 1 rad m<sup>-2</sup>. RMFIT applies Faraday rotation correction for each trial RM and

 $<sup>^2</sup>$  Xu et al. (2025) reported a 26.24  $\pm\,0.02$  day RM periodicity with a significance > 5.9  $\sigma$  in FRB 20201124A when our results is nearly finished.

selects the RM that maximizes the linear polarization as the final measurement. Please see more details in (Li et al. 2025). The updated RM values are presented as blue dots in Figure 1.

### 3. PERIODICITY EXAMINATIONS

In order to explore the possible periodicity of FRB 20220529, we examine the periodicity using the RM series described in Section 2. As reported in Li et al. (2025), FRB 20220529 experienced an abrupt change and prompt recovery of RM at the end of 2023, reaching  $\sim$  20  $\sigma$  of the RM baseline (from -300 rad m<sup>-2</sup> to +300 rad m<sup>-2</sup>). We therefore exclude those pulses within the "RM flare" epoch and with  $RM > 300 \text{ rad m}^{-2}$  in our periodicity studies, specifically 60290 < MJD < 60310 as they are inconsistent with any periodic pattern. Due to the fluctuations of the magnetized plasma, the RMs exhibit significant daily variations. We thus binned the RMs within one day by RM = RM(MJD). The resulting daily-binned RMs are plotted as pink points in Figure 1. The periodicity examinations with the Lomb-Scargle Periodogram and phase-folding analysis are presented in Section 3.1 and 3.2, respectively.

### 3.1. Lomb-Scargle Periodogram

The Lomb-Scargle periodogram (Lomb 1976; Scargle 1982) is a powerful method for detecting periodic signals in unevenly sampled time-series data. It estimates spectral power over a range of trial periods, identifying periodicities by evaluating their statistical significance. The spectral power is defined as

$$P_{LS}(\omega) = \frac{1}{2} \left\{ \frac{\left[\sum_{i} RM_{i} \cos \omega (t_{i} - \tau)\right]^{2}}{\sum_{i} \cos^{2} \omega (t_{i} - \tau)} + \frac{\left[\sum_{i} RM_{i} \sin \omega (t_{i} - \tau)\right]^{2}}{\sum_{i} \sin^{2} \omega (t_{i} - \tau)} \right\},$$
(1)

where  $\omega$  is the angular frequency, RM<sub>i</sub> is the observed RM value of the *i*-th time point,  $t_i$  is the time of the *i*-th data point, and  $\tau$  is specified for each  $\omega$  to ensure the periodogram's invariance under time translations:

$$\tau = \frac{1}{2\omega} \tan^{-1} \left( \frac{\sum_{i} \sin 2\omega t_{i}}{\sum_{i} \cos 2\omega t_{i}} \right), \tag{2}$$

where i ranges from 1 to N in the summation. N is the total number of RM points. By normalizing the spectral power, the algorithm quantifies the likelihood of periodicity and determines the most prominent candidate.

This method is particularly well-suited for astronomical time-domain studies, where observations are often sparse and irregularly sampled. Unlike the classical Fourier transform, the LSP effectively handles data gaps and provides unbiased estimates of periodic signals (VanderPlas 2018). We implement the LSP us-

ing the LombScargle class from the astropy package<sup>3</sup>. We compute the false alarm probability (FAP), which quantifies the likelihood that an observed peak in the power spectrum arises purely from random noise under the null hypothesis. The power threshold corresponding to a given FAP is determined using the false\_alarm\_probability method of the LombScargle class.

The results of FRB 20220529 are shown in upper left panel of Figure 2. Using a FAP threshold of  $10^{-4}$ , we identified the most significant period as  $P = 199^{+15}_{-18}$  days. The uncertainty is estimated by resampling the data with a bootstrap method here. In addition, we performed simulations by bootstrap resampling the measured RM values while preserving their temporal arrival times. This method accounts for both the irregular sampling and measurement uncertainties inherent in the original data. We found that in  $10^6$  simulations, the probability of obtaining a peak matching the observed one was about  $6.1 \times 10^{-5}$ , corresponding to a signal-tonoise ratio (SNR) of  $4.2~\sigma$ . The simulation results are shown in upper right panel of Figure 2.

### 3.2. Phase Folding method

We apply the classical and effective method—the phase folding algorithm—to analyze the RM variations of FRB 20220529. Given the about 800 days of monitoring data, which are unevenly sampled and require consideration of the RM values, the phase folding method is expected to provide a more reliable analysis to some extent. Based on the principle of phase folding, we first assume an initial trial period  $P_0$ . The N RM values in the sample, corresponding to their respective TOAs, will then be folded into  $N/P_0$  periods. Typically, the first data point is considered as the zero-point  $t_0$ . Subsequently, the phase of the i-th RM can be calculated as:

$$\phi_i = \frac{(t_i - t_0) \mod P_0}{P_0},\tag{3}$$

where  $t_i$  is the time of the *i*-th RM value, and  $P_0$  is the assumed trial period.

As for how to quantitatively assess whether  $P_0$  is a potential true period, we decide to use the classical  $\chi^2$  test. This is based on the reasoning that if the RM values exhibit a specific period, then after folding, their distribution should significantly deviate from a random distribution in the phase space. The  $\chi^2$  value could be calculated as:

$$\chi^2 = \sum_{j=1}^n \frac{(O_j - E)^2}{E},\tag{4}$$

where the n is the total number of bins for a particular period  $P_0$ , the  $O_j$  is the real RM value in j-th bin, and

<sup>&</sup>lt;sup>3</sup> https://docs.astropy.org/en/stable/timeseries/lombscargle.html

Table 1. FAST observations and the bursts detected after September 5th, 2024

Date	Start MJD	Duration	$N_{ m FRB}$	MJD	RM
		(minutes)			$(rad m^{-2})$
2024-10-04	60587.75208	20	9	60587.7539552	$-129\pm20$
				60587.7555989	-
				60587.7555993	-
				60587.7567309	$-142\pm5$
				60587.7606994	$-146 \pm 3$
				60587.7613663	$-121\pm 6$
				60587.7612692	$-137.0\pm0.1$
				60587.7643518	-
				60587.7650848	$-128\pm31$
2024-10-17	60600.72292	20	1	60600.7339299	$-292\pm23$
2024-11-01	60615.58611	20	2	60615.5896371	$-261 \pm 34$
				60615.5880082	$-308 \pm 94$
2024-11-21	60635.57153	20	0	-	-
2024-12-03	60647.54167	20	0	-	-
2024-12-19	60663.52986	20	0	-	-
2025-01-01	60676.40625	20	0	-	-
2025-01-05	60680.50972	30	0	-	-
2025-01-29	60704.28611	20	0	-	-
2025-02-10	60716.35486	20	0	-	-
2025-02-22	60728.27083	20	1	60728.2788674	$-105\pm25$
2025-03-09	60743.23472	20	0	-	-
2025-03-22	60756.20903	20	0	-	-

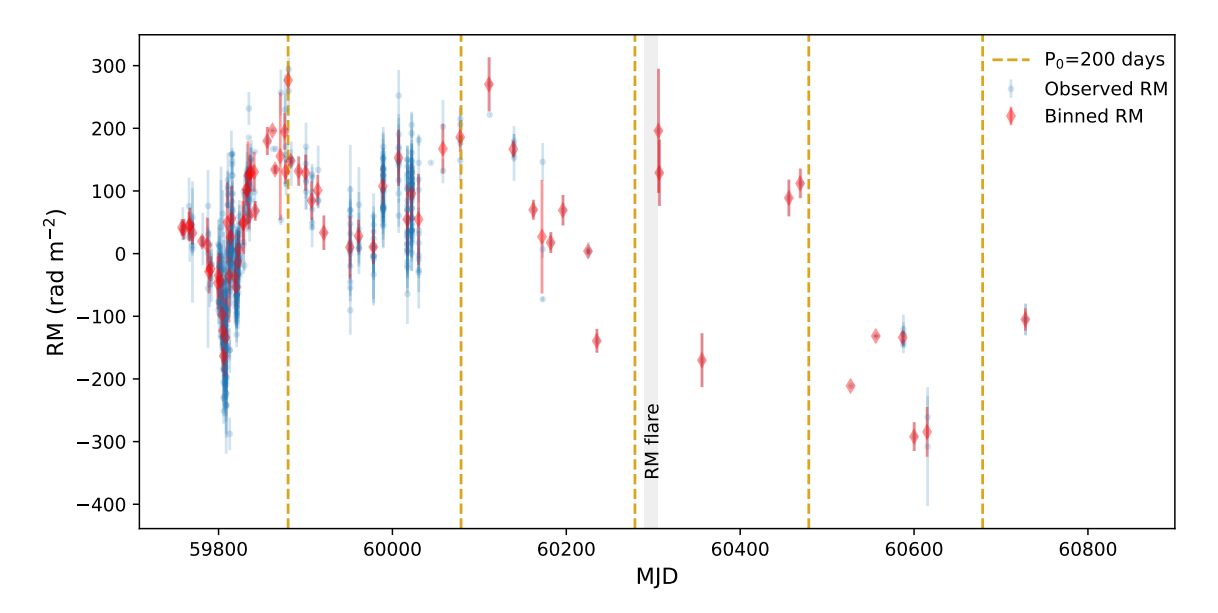


**Figure 1.** RM evolution of FRB 20220529. The blue points represent the detected RM values with their uncertainties. The red points correspond to the daily-binned RM values. The orange lines mark the phases corresponding to the peak of the 200-day period, approximately at phase 0.25.

E is the expected value assuming the RM values are ran-

domly and uniformly distributed across the entire phase

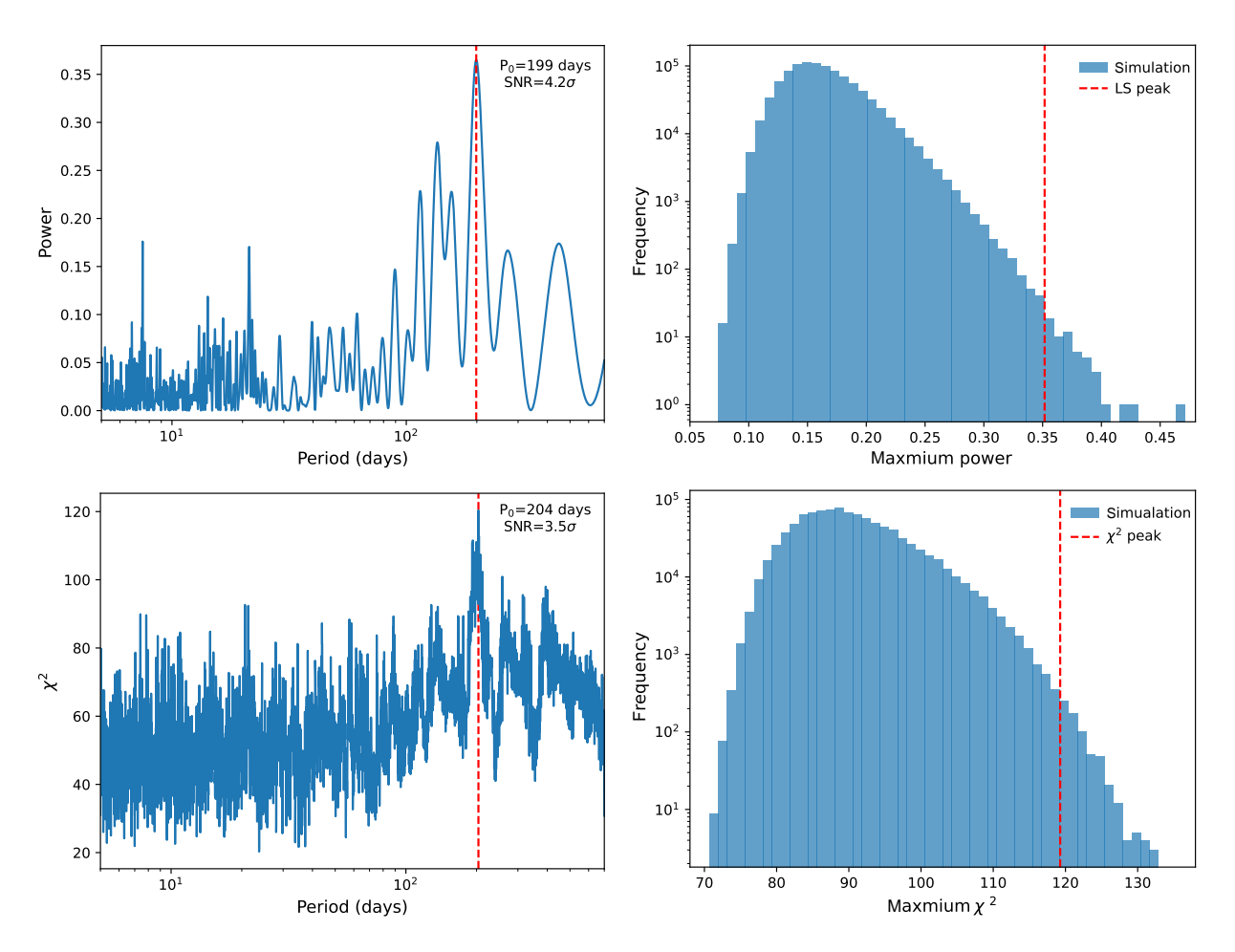


Figure 2. Results of Periodicity examinations. Upper Left: LSP of RM variations for FRB 20220529, derived from FAST observations. The red dashed line marks the most significant peak detected at 199 days. The x-axis of the plot is logarithmic. Upper right: Simulation results of the LSP. The red dashed line represents the maximum power obtained with the observed RM. In the simulation, RM values were randomly selected and assigned to the TOA before applying the LSP.  $10^6$  simulations were performed. The probability of obtaining a maximum power greater than or equal to the observed maximum power is  $6.1 \times 10^{-5}$ . Lower Left: Results of phase folding analysis. The red dashed line indicates the period corresponding to the maximum  $\chi^2$  value, which is 204 days. The x-axis of the plot is logarithmic. Lower Right: Simulation results of phase folding analysis.  $10^6$  simulations were performed. The probability of obtaining a maximum  $\chi^2$  greater than or equal to the observed maximum  $\chi^2$  is  $8.45 \times 10^{-4}$ .

space. Typically, a large value of  $\chi^2$  suggests that  $P_0$  is a plausible candidate for the period of the burst activity, whereas a small  $\chi^2$  value implies that  $P_0$  is unlikely to correspond to the intrinsic period. By systematically varying  $P_0$  across a range of potential period values, we can determine the true period, if it exists, through statistical testing.

In our work, we bin the RM values of daily bursts into a single value for each day. We then test periods within the range of 1 to 700 days, dividing each trial period into 12 bins. This approach leads to the identification of a best-fit period of  $204^{+16}_{-27}$  days. The uncertainty of the period is derived using a bootstrap resampling method. The corresponding  $\chi^2$  distribution is shown in the lower left panel in Figure 2. Finally, we also perform an MCMC simulation to determine the SNR of the iden-

tified period. For each simulation, we compute the  $\chi^2$  value, and record the maximum  $\chi^2$ . After conducting  $10^6$  simulations, we find that the probability of obtaining a maximum  $\chi^2$  matching the observed one is about  $8.4 \times 10^{-4}$ , corresponding to SNR =  $3.5 \sigma$ . And the result of simulation is shown in the lower right panel of Figure 2.

We fold the RM evolution with a 200-day period and present the folded RM distribution as a function of phases in Figure 3. The folded RM evolution is fitted with a sin function. The best-fitted function is

$$RM = RM_0 + RM_A \sin\left(2\pi \frac{t - MJD_0}{P}\right).$$
 (5)

with the best-fitting parameters  $\rm MJD_0=59828,\ RM_A=76.97\ rad\ m^{-2}$  and  $\rm RM_0=83.53\ rad\ m^{-2}.$  We

label the peaks as verticle yellow dashed line in Figure 1. It can be seen that the predicted peaks generally match the four peaks in the RM evolution.

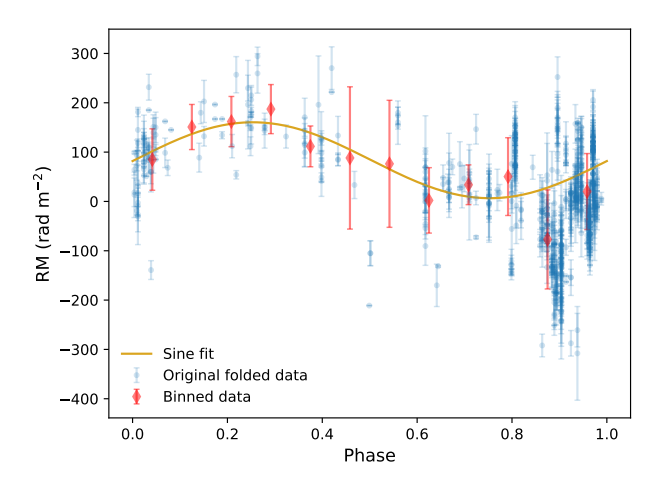


**Figure 3.** Phase-folded RM variations with a 200-day period. The blue points represent the observed RM values and their uncertainties. The red points show the averaged RM values within each phase bin. The orange line depicts the fit result to a sine function.

#### 4. DISCUSSION

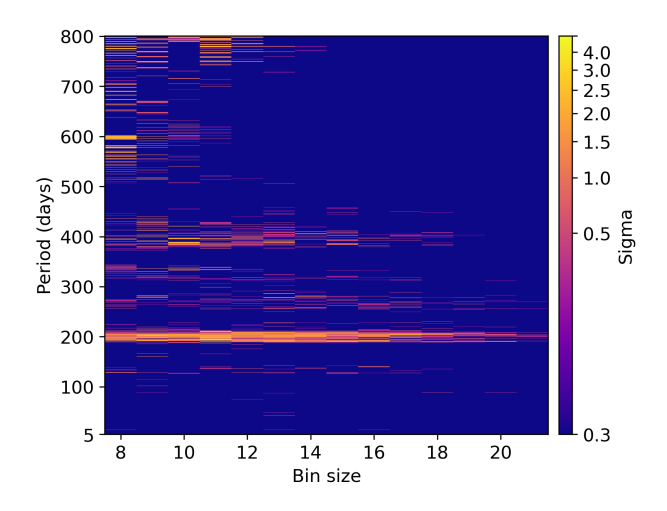


Figure 4. Significance for different bin sizes and periods in phase-folding periodicity search. The x-axis represents the bin size, and the y-axis shows the period. The color intensity indicates the corresponding significance, which reflects the significance of the periodicity detection for each trial. It is evident that periods around  $\sim 200$  days are relatively significant for reasonable bin sizes.

# 4.1. Effect of the "RM flare"

In our periodic studies, we excluded the data with  $|{\rm RM}| > 300~{\rm rad~m^{-2}}$  within the "RM flare" epoch, specifically 60290 < MJD < 60310. We choose 300 rad m<sup>-2</sup> as the upper limit since it is generally 3  $\sigma$  of the RM standard deviation and includes nearly all other data. Still, we tested the results with all the data, including "RM flare". The LSP still presents the  $\sim$  200-day periodicity as the most prominent one, with a significance of 4.5  $\sigma$ . In contrast, the phase-folding method is more strongly affected by the inclusion of the RM flare. It reveals that the LSP could deal with outliers much better than phase-folding method. Given that the RM flare is clearly not part of the underlying periodic RM evolution, it is more appropriate to exclude this segment from the analysis.

### 4.2. Limitation of the Lomb-Scargle periodogram

Despite the capability of the LSP to handle unevenly sampled data, it also has drawbacks. Specifically, it has the tendency to generate spurious peaks and obscure genuine periodic signals, thereby compromising the accuracy of periodicity analysis.

Firstly, the LSP is based on the assumption that the underlying signal is sinusoidal. Consequently, its detection capability for non-sinusoidal periodic signals or those containing small-scale structures is significantly reduced. As illustrated in Figure 1, the RM evolution does not follow a standard sinusoidal pattern and exhibits irregular variations, such as the peak near MJD 60000. These deviations from the sinusoidal form give rise to multiple peaks in the LSP. For instance, a prominent secondary peak is observed at approximately the 130-day period. According to Monte Carlo simulations, this peak has a statistical significance of 3.0  $\sigma$ . Furthermore, the RM evolution around MJD 59800 resembles a compressed portion of a sine wave and displays numerous minor peaks. These minor peaks in the RM data generate multiple small peaks in the LSP, such as the peak around the 20-day period. The cumulative effect of these peaks in the RM curve leads to fluctuations in the LSP.

Secondly, the LSP is sensitive to irregular sampling. As illustrated in Figure 1, the sampling rate before MJD 60050 is significantly higher than that after it. This is primarily due to the increased FRB activity. As reported in Li et al. (2025), FRB 20220529 exhibited two active bursting epochs around MJD 59800 and MJD 60000. Moreover, the community typically schedules intensive observations during epochs of high burst rates, further enhancing the unevenness of the sampling. An unbinned analysis tends to downplay the contributions of data points collected during epochs of low FRB activity, especially after MJD 60050. In addition, RM is inherently subject to strong fluctuations. Since periodic studies require capturing the long-term trends, we binned RM values on a daily basis before performing the periodicity analysis. In order to assess the impact of the binning, we also conducted a periodicity analysis using unbinned RM data. The LSP reveals that the peak near 198 days persists, while the second peak in the upper left panel of Figure 2 becomes more pronounced. This is a result of uneven sampling. It is evident that daily binning of RM data provides a clearer depiction of periodic behavior over extended timescales. Although an evenly sampled RM dataset could ideally improve the periodicity analysis, achieving this is challenging. Even with regularly scheduled observations, it is inherently constrained by the irregular nature of FRB activity.

### 4.3. Limitation of the phase folding method

When using the phase folding method to search for periodicity, we initially adopted a bin size of 12 to calculate the  $\chi^2$ . Here we tested the impact of different bin sizes on the results. The significance for different bin size and periods are presented in Figure 4. It shown that with bin sizes from 8 to 22, the periods around 200 have significance larger than 3  $\sigma$ . The results indicate that within a reasonable range, the bin size does not significantly affect the periodicity detection. It is important to note that the significance (in terms of sigma) in Figure 4 represents the relative strength of the trial periods, rather than the actual SNR of the detected periodicity. The final result presented in Figure 2, obtained with nbin=12, shows the most significant periodicity.

### 4.4. Effect of sampling

In order to investigate whether the periodic signals detected in the RM time series are dominated by the sampling process, we further examined the periodicity of the burst rate of the pulses. The LSP of the pulses is presented as the blue line in Figure 5, with the result of the RM evolution overplotted as the orange line. To make a direct comparison between the results of the burst rate and RM, we plot the FAP instead of power here. It turns out that there is also a peak at approximately 200 days in the LSP of the burst rate. Although the peak hints a tentative  $\sim 200$ -day periodic activity, it is not statistically significant. The FAP values for the RM dataset at  $P_0 = 199$  days show significantly higher statistical confidence (>  $3\sigma$ ) compared to the periodicity results of the burst rate, which remain consistent with noise (SNR  $< 3\sigma$ ). Thus, the periodic evolution of the RM is neither dominated by the sampling process nor by the burst rate. The periodic evolution of the RM is more likely inherent to the system, if it is not merely coincidental. We want to note that, during the active bursting epochs, MJD around 59800 and 60000, the fold phases of RM are around 0.86. It indicates an larger burst rate when the RM is small. However, it is not significant since there is no other bursting phases detected besides them.

# 4.5. Physical implications

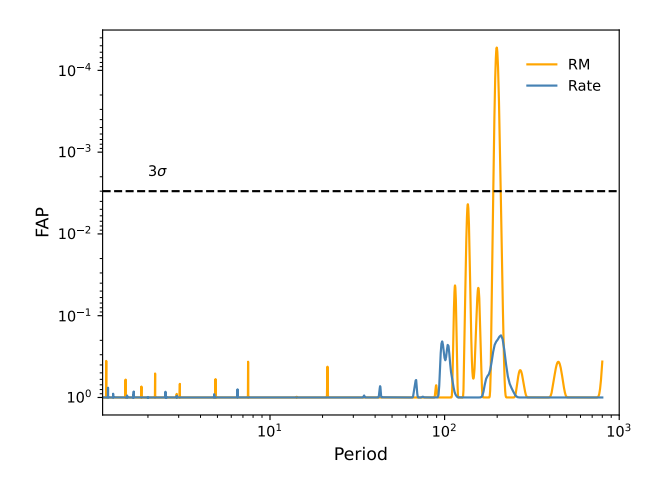


Figure 5. False Alarm Probability versus trial period in LSP. Orange points show FAP values for each trial period in the RM periodicity search, while blue points denote results from the Burst Rate periodicity analysis. Gray dashed lines indicate statistical significance thresholds corresponding to  $3\sigma$  and  $5\sigma$  confidence levels. The y-axis is inverted, with FAP values decreasing from bottom to top.

The possible 200-day periodic RM evolution revealed in our analysis carries significant implications for understanding the origin of FRBs. As a convolution of the electron density and magnetic field in the line of sight, the observed RM of an FRB from a redshift z is attributed to various plasma components,  $RM_{obs} = RM_{ion} + RM_{MW} + RM_{IGM} + RM_{host}/(1 +$  $(z)^2 + RM_{loc}/(1+z)^2$ . Here, RM<sub>ion</sub> denotes the contribution from the Earth's ionosphere, typically on the order of 0.1-1 rad m<sup>-2</sup> (Mevius 2018). RM<sub>MW</sub> represents the contribution from the interstellar medium within the Milky Way. In the case of FRB 20220529, this value is approximately  $-35 \text{ rad m}^{-2}$  (Oppermann et al. 2015). RM<sub>IGM</sub> accounts for the contribution from the intergalactic medium, which is typically  $< 10 \text{ rad m}^{-2}$ (Akahori et al. 2016). RM<sub>host</sub> is the contribution from the interstellar medium within the FRB's host galaxy, potentially comparable in magnitude to that of the Milky Way. Lastly, RM<sub>loc</sub> signifies the contribution from the local plasma in the immediate vicinity of the FRB source. Therefore, an observed RM with an absolute value  $> 10^2$  rad m<sup>-2</sup> is expected to be mainly contributed by the local plasma RM<sub>loc</sub>. In addition, the variation timescales of interstellar and intergalactic medium are expected to be long. The possible RM variation observed here is expected to be a result of the local magneto-ionic environment.

It is natural to consider that the periodic evolution of the RM is generated by the orbital configuration of a binary system. If the FRB progenitor resides in a binary system, the stellar winds from a massive/giant star companion would contribute to the RM (Wang et al. 2022; Yang et al. 2023). Thus, the orbital motion or the

dynamic evolution of the wind would result in RM variations, and the RM variation due to the orbital motion should have the same period as the orbital period. The binary system model is further supported by the "RM flare" reported in (Li et al. 2025). In this case, the "RM flare" is more likely to originate from a corona mass ejection (CME) from the companion or a disk, because the orbital configuration producing the "RM flare" requires an orbital period > 1000 days and an eccentricity > 0.9. The binary model is also consistent with the peak at approximately 200 days in the LSP of the burst rate, which indicates tentative periodic activity that aligns with the periodic RM evolution.

Also, the periodic RM variation could also arise from magnetized outflows or a disk associated with a massive black hole (Zhang 2018; Yang et al. 2023). If the orbit of the FRB source is elliptical, a large RM variation would occur near the periastron and remain nearly constant far away from the periastron. A periodic evolution of RM variation could result from the orbital motion of the FRB sources. However, FRB 20220529 is not located at the center of its host galaxy. The distance between FRB 20220529 and the center of the host galaxy exceeds the half-light radius of the host. Moreover, outflows from a massive black hole typically induce an RM of  $\gtrsim 10^4 \text{ rad m}^{-2}$ , whereas the RM amplitude observed for FRB 20220529 in this study is around 100 rad  $m^{-2}$ . According to Equation (50) of Yang et al. (2023), a black hole with a mass of  $10^3~M_{\odot}$  would produce an RM of  $\sim 100 \text{ rad m}^{-2}$ , indicating that an intermediate mass black hole may also account for the periodic RM evolution here. However, since the FRB progenitor is widely believed to be a neutron star, an intermediate-mass black hole scenario would imply a black hole-neutron star system. Such a scenario would necessitate additional components to explain the black hole's outflow or disk, making the model somewhat complex.

At last, if a Faraday screen with an inhomogeneous medium is present near the FRB source, the relative motion between the FRB source and the screen would induce random RM variations. These variations could be quantified using the structure function. Li et al. (2025) reveals that the structure function for the RM of FRB 20220529 is consistent with other repeating FRBs, although slightly shallower. Given significance levels of 4.2  $\sigma$  and 3.5  $\sigma$  for the 200 days periodicity, based on the LSP and phase-folding analysis, respectively, we cannot rule out the possibility that the observed signal arises from random fluctuations. Longer-term monitoring is still required to confirm or refute the tentative periodicity identified here. Moreover, although precession of the neutron star's spin or magnetic axis may induce a peri-

odic modulation in burst rate, they do not typically result in periodic RM evolution because the medium along the line of sight does not change much. We thus do not discuss precession in detail here.

#### 5. CONCLUSION

In this paper, we present an investigation of the periodicity of FRB 20220529 using three years of monitoring data from FAST telescope. The RM evolution exhibits a potential periodic modulation with a period of P =  $199^{+15}_{-18}$  days (LSP), P =  $204^{+16}_{-27}$  days (Phase Folding). The statistical significance is 4.2  $\sigma$  determined by the LSP and 3.5  $\sigma$  from phase-folding analysis. While the discrepancy between the two methods may arise from algorithmic sensitivity to non-sinusoidal signals or uneven sampling, their mutual consistency supports the case for periodicity. An examination of burst rate variability also suggests a similar timing feature, though much less significant.

We discussed three plausible scenarios: (1) Binary Orbital Motion: A binary system with a massive/giant star companion would induce RM periodicity through orbital motion. However, current data insufficiently constrain the companion's mass or orbital parameters. (2) Massive Black hole: An intermediate-mass black hole with outflows or an accretion disk would induce periodic RM evolution similar to that identified here. However, this scenario requires additional components to produce the outflow/disk, making the system more complex. (3) Turbulence: Variations in an inhomogeneous medium along the line of sight would produce random RM variations. Although this scenario is not statistically preferred, it can not be fully ruled out. The possible periodic RM evolution identified here requires extended monitoring to validate it.

## ACKNOWLEDGEMENTS

YL thanks Qiang Yuan for helpful discussion. YFL thanks Tiancong Wang for helpful discussion. This work is partially supported by the Natural Science Foundation of China (Grant Nos. 12321003, 12041306, 12103089,12393813), the National Key Research and Development Program of China (2022SKA0130100), National Key R&D Program of China(2024YFA1611704), the Natural Science Foundation of Jiangsu Province (Grant No. BK20211000), International Partnership Program of Chinese Academy of Sciences for Grand Challenges (114332KYSB20210018), the CAS Project for Young Scientists in Basic Research (Grant No. YSBR-063), the CAS Organizational Scientific Research Platform for National Major Scientific and Technological Infrastructure: Cosmic Transients with FAST.

# REFERENCES

Akahori, T., Ryu, D., & Gaensler, B. M. 2016, ApJ, 824, 105, doi: 10.3847/0004-637X/824/2/105 Amiri, M., Andersen, B., Bandura, K., et al. 2020, Nature, 582, 351–355, doi: 10.1038/s41586-020-2398-2

- Anna-Thomas, R., Connor, L., Dai, S., et al. 2023, Science, 380, 599, doi: 10.1126/science.abo6526
- Bethapudi, S., Spitler, L. G., Li, D. Z., et al. 2025, A&A, 694, A75, doi: 10.1051/0004-6361/202452221
- Braga, C. A., Cruces, M., Cassanelli, T., et al. 2025, A&A, 693, A40, doi: 10.1051/0004-6361/202451905
- Chime/Frb Collaboration, Andersen, B. C., Bandura, K., et al. 2023, ApJ, 947, 83, doi: 10.3847/1538-4357/acc6c1
- Cruces, M., Spitler, L. G., Scholz, P., et al. 2020, Monthly Notices of the Royal Astronomical Society, 500, 448–463, doi: 10.1093/mnras/staa3223
- Hilmarsson, G. H., Michilli, D., Spitler, L. G., et al. 2021,The Astrophysical Journal Letters, 908, L10,doi: 10.3847/2041-8213/abdec0
- Ioka, K., & Zhang, B. 2020, ApJL, 893, L26, doi: 10.3847/2041-8213/ab83fb
- Katz, J. I. 2016, ApJ, 826, 226, doi: 10.3847/0004-637X/826/2/226
- Levin, Y., Beloborodov, A. M., & Bransgrove, A. 2020, The Astrophysical Journal Letters, 895, L30, doi: 10.3847/2041-8213/ab8c4c
- Li, D., Wang, P., Zhu, W. W., et al. 2021, Nature, 598, 267, doi: 10.1038/s41586-021-03878-5
- Li, Y., Zhang, S. B., Yang, Y. P., et al. 2025, An active repeating fast radio burst in a magnetized eruption environment. https://arxiv.org/abs/2503.04727
- Lomb, N. R. 1976, Ap&SS, 39, 447, doi: 10.1007/BF00648343
- Lorimer, D. R., Bailes, M., McLaughlin, M. A., Narkevic,
   D. J., & Crawford, F. 2007, Science, 318, 777,
   doi: 10.1126/science.1147532
- Lyubarsky, Y. 2008, ApJ, 682, 1443, doi: 10.1086/589435
- Mevius, M. 2018, RMextract: Ionospheric Faraday Rotation calculator, Astrophysics Source Code Library, record ascl:1806.024
- Michilli, D., Seymour, A., Hessels, J. W. T., et al. 2018, Nature, 553, 182–185, doi: 10.1038/nature25149
- Niu, C. H., Aggarwal, K., Li, D., et al. 2022, Nature, 606, 873, doi: 10.1038/s41586-022-04755-5
- Oppermann, N., Junklewitz, H., Greiner, M., et al. 2015, A&A, 575, A118, doi: 10.1051/0004-6361/201423995
- Pal, A. 2025, arXiv e-prints, arXiv:2502.11215, doi: 10.48550/arXiv.2502.11215
- Pastor-Marazuela, I., Connor, L., van Leeuwen, J., et al. 2021, Nature, 596, 505, doi: 10.1038/s41586-021-03724-8

- Petroff, E., Keane, E. F., Barr, E. D., et al. 2015, Monthly Notices of the Royal Astronomical Society, 451, 3933–3940, doi: 10.1093/mnras/stv1242
- Platts, E., Weltman, A., Walters, A., et al. 2019, PhR, 821,1, doi: 10.1016/j.physrep.2019.06.003
- Rajwade, K. M., Mickaliger, M. B., Stappers, B. W., et al. 2020, Monthly Notices of the Royal Astronomical Society, 495, 3551, doi: 10.1093/mnras/staa1237 Ransom, S. M. 2001
- Scargle, J. D. 1982, ApJ, 263, 835, doi: 10.1086/160554
- Spitler, L. G., Scholz, P., Hessels, J. W. T., et al. 2016, Nature, 531, 202, doi: 10.1038/nature17168
- Sridhar, N., Metzger, B. D., Beniamini, P., et al. 2021, ApJ, 917, 13, doi: 10.3847/1538-4357/ac0140
- The CHIME/FRB Collaboration, :, Andersen, B. C., et al. 2019, arXiv e-prints. https://arxiv.org/abs/1908.03507
- Thornton, D., Stappers, B., Bailes, M., et al. 2013, Science, 341, 53–56, doi: 10.1126/science.1236789
- VanderPlas, J. T. 2018, ApJS, 236, 16, doi: 10.3847/1538-4365/aab766
- Wada, T., Ioka, K., & Zhang, B. 2021, ApJ, 920, 54, doi: 10.3847/1538-4357/ac127a
- Wang, F. Y., Zhang, G. Q., Dai, Z. G., & Cheng, K. S. 2022, Nature Communications, 13, 4382, doi: 10.1038/s41467-022-31923-y
- Xu, H., Niu, J. R., Chen, P., et al. 2022, Nature, 609, 685–688, doi: 10.1038/s41586-022-05071-8
- Xu, J., Xu, H., Guo, Y., et al. 2025, Periodic variation of magnetoionic environment of a fast radio burst source. https://arxiv.org/abs/2505.06006
- Yang, Y.-P., Xu, S., & Zhang, B. 2023, MNRAS, 520, 2039, doi: 10.1093/mnras/stad168
- Zhang, B. 2018, ApJL, 854, L21, doi: 10.3847/2041-8213/aaadba
- 2023, Reviews of Modern Physics, 95, 035005, doi: 10.1103/RevModPhys.95.035005
- Zhang, Y.-K., Li, D., Zhang, B., et al. 2023, FAST Observations of FRB 20220912A: Burst Properties and Polarization Characteristics. https://arxiv.org/abs/2304.14665
- Zhao, Z. Y., Zhang, G. Q., Wang, F. Y., & Dai, Z. G. 2023,The Astrophysical Journal, 942, 102,doi: 10.3847/1538-4357/aca66b
- Zhou, D., Han, J. L., Zhang, B., et al. 2025, arXiv e-prints, arXiv:2504.11173, doi: 10.48550/arXiv.2504.11173
- Zhou, D. J., Han, J. L., Zhang, B., et al. 2022, Research in Astronomy and Astrophysics, 22, 124001, doi: 10.1088/1674-4527/ac98f8